# Cylindrical cellular geometry ensures fidelity of division site placement in fission yeast

**Mithilesh Mishra[1,*], Yinyi Huang[2,*], Pragya Srivastava[3,*], Ramanujam Srinivasan[2,*], Mayalagu Sevugan[1], Roie Shlomovitz[4], Nir Gov[4], Madan Rao[3,5,‡] and Mohan Balasubramanian[1,2,6,‡]**

[1]Temasek Life Sciences Laboratory, 117604, Singapore
[2]Mechanobiology Institute, National University of Singapore, 117411, Singapore
[3]Raman Research Institute, Bangalore 560080, India
[4]Department of Physics, Weizmann Institute, Rehovot, 76100, Israel
[5]National Centre for Biological Sciences (TIFR), Bangalore 560065, India
[6]Department of Biological Sciences, National University of Singapore, 117543, Singapore

*These authors contributed equally to this work
‡Author for correspondence (mohan@tll.org.sg; madan@ncbs.res.in)

*Accepted 25 March 2012*
*Journal of Cell Science 125, 3850–3857*

*doi: 10.1242/jcs.103788*

## Summary

Successful cytokinesis requires proper assembly of the contractile actomyosin ring, its stable positioning on the cell surface and proper constriction. Over the years, many of the key molecular components and regulators of the assembly and positioning of the actomyosin ring have been elucidated. Here we show that cell geometry and mechanics play a crucial role in the stable positioning and uniform constriction of the contractile ring. Contractile rings that assemble in locally spherical regions of cells are unstable and slip towards the poles. By contrast, actomyosin rings that assemble on locally cylindrical portions of the cell under the same conditions do not slip, but uniformly constrict the cell surface. The stability of the rings and the dynamics of ring slippage can be described by a simple mechanical model. Using fluorescence imaging, we verify some of the quantitative predictions of the model. Our study reveals an intimate interplay between geometry and actomyosin dynamics, which are likely to apply in a variety of cellular contexts.

**Key words:** Actinomysin ring, Cell geometry, Cell division

## Introduction

Cytokinesis in many organisms, from yeasts to human, involves the function of a contractile actomyosin ring (Balasubramanian et al., 2004). Forces generated upon interaction between F-actin and myosin II leads to the closure of the actomyosin ring and the division of the cytoplasm. The assembly, stable positioning and proper constriction of the contractile actomyosin ring on the cell surface are necessary sequential steps in the successful execution of cytokinesis and have been investigated in detail (Balasubramanian et al., 2004; Wolfe and Gould, 2005; Pollard and Wu, 2010). However, whether the shape of the cell itself plays a role in the regulation of aspects of cytokinesis has not been investigated.

In recent years the fission yeast *Schizosaccharomyces pombe* has emerged as an attractive model for the study of cytokinesis, since it divides using an actomyosin based contractile ring and since various experimental approaches and methods are easily applied in this organism. Fission yeast cells are cylindrical in shape and divide by fission at the medial region of the cell to produce daughters of equal size. In fission yeast, the cytokinetic actomyosin ring is assembled upon entry into mitosis and constricts when mitotic spindle breaksdown upon completion of mitosis. Actomyosin ring constriction is tightly coupled with the assembly of new membranes and the division septum. In fission yeast, actomyosin ring assembly and function requires evolutionarily conserved molecules such as F-actin (Schroeder, 1973), myosin II (Maupin and Pollard, 1986), formin (Goode and Eck, 2007), members of the F-BAR family of proteins (Fankhauser et al., 1995; Aspenström, 2009), and anillin-related proteins (D'Avino, 2009). Previous studies in fission yeast have shown that a compromise of the cylindrical morphology of cells leads to defects in septum placement underscoring an interplay between morphogenesis and cytokinesis, although the mechanisms have not been investigated (Ge et al., 2005). Recently, dependence of the cell division site on cellular geometry has also been inferred from work in sea urchins (Minc et al., 2011).

In this study, we use the fission yeast *S. pombe* as a model to investigate the role of cell geometry and mechanics on the stable positioning and constriction of the actomyosin ring. We find that actomyosin rings located in regions where the geometry is locally spherical do not undergo normal constriction but rather undergo a sliding behavior, whereas rings assembled in cellular regions with a cylindrical geometry support proper septation. This interplay between the dynamics of actomyosin rings and cell geometry can be understood using a simple mechanical model. We verify the assumptions and predictions of this model from fluorescence images of the actomyosin ring, and discuss its biological implications.

## Results

Wild-type (WT) fission yeast cells have cylindrical shapes and hemispherical ends, and divide medially through the proper assembly, positioning and contraction of the actomyosin ring (Marks et al., 1986; Chang and Nurse, 1996; Le Goff et al.,

1999b). To assess actomyosin ring behavior in cells of altered geometry, we first generated spherical WT cells (referred to as spheroplasts) by removal of the cell wall in an osmotically stabilized environment. We chose to work with spheroplasts rather than spherical mutants, because potential defects in cytokinesis in spherical mutants could be attributed to possible loss of protein function instead of geometry.

To visualize the actomyosin ring, we first expressed a GFP-fused version of myosin II regulatory light chain, Rlc1p–GFP, or the calponin-homology domain of IQGAP-related protein Rng2p in the WT cells that were used for the generation of spheroplasts (Naqvi et al., 2000; Karagiannis et al., 2005). In some instances we simultaneously imaged the behavior of mCherry-tubulin to correlate actomyosin ring dynamics with the cell cycle. Wild-type spheroplasts were prepared by treatment of cells with an enzyme cocktail that disrupts the cell wall, and maintained in a medium containing 0.8 M sorbitol to prevent osmolysis. We found that in all cases, spheroplasts without (or with undetectable levels of) a cell wall (as judged by aniline blue staining; data not shown) successfully assembled actomyosin rings (Fig. 1A,B). Unlike in intact cells, these rings assembled late in anaphase after the breakdown of the spindle (supplementary material Fig. S1A). In most cases we observed that once assembled, the actomyosin rings in spheroplasts were mechanically unstable; while they maintained their integrity as a ring, they systematically slid along the cortex towards the poles (Fig. 1A,B; supplementary material Movies 1–8), simultaneously shrinking in radius. The anillin-related protein Mid1p localized to the early arcs or rings. However, Mid1p signals were not detected in mature and sliding rings as in intact cells (supplementary material Fig. S1B). The absence of fission could have been because these spheroplasts were osmotically tense. The qualitative and quantitative (as we

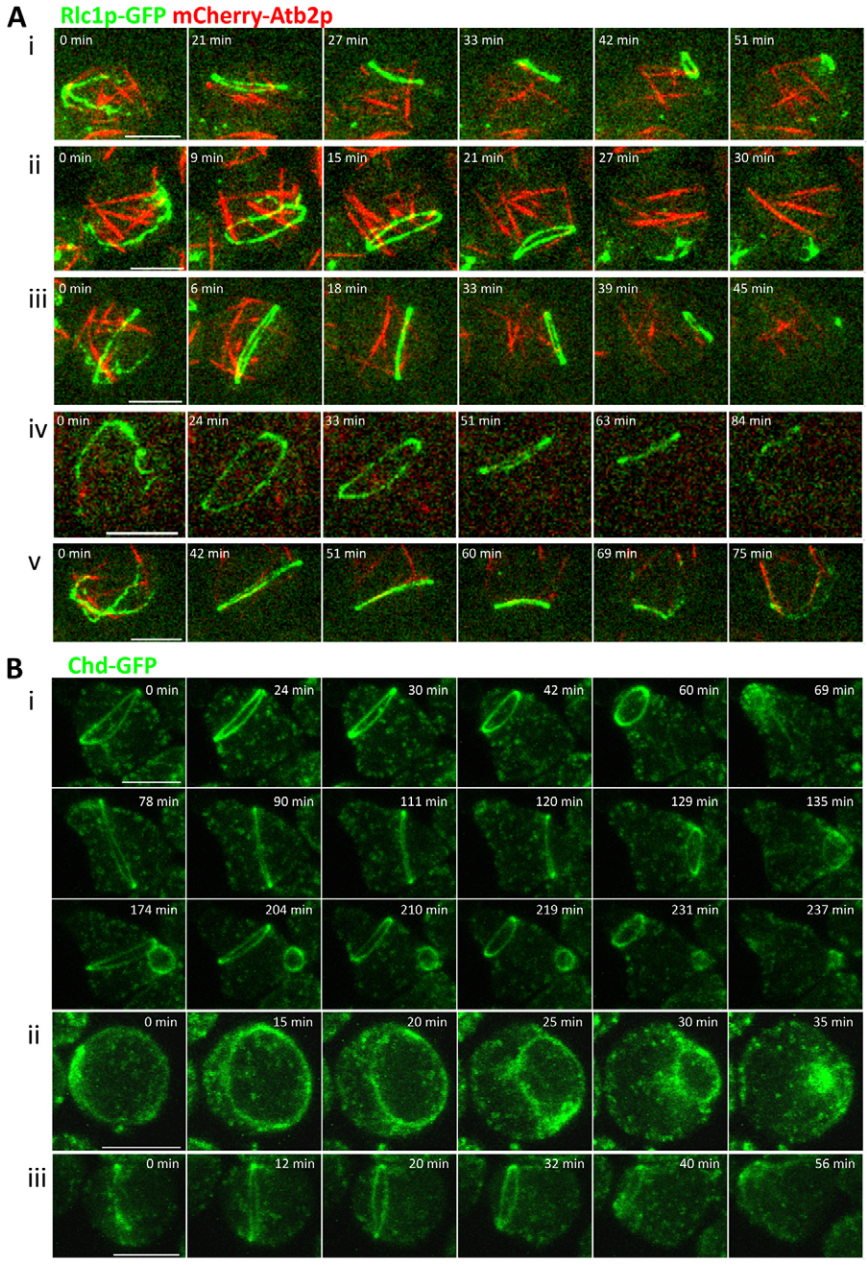


**Fig. 1. Actomyosin rings formed in spherical or conical protoplasts slide along the surface instead of ingressing centripetally upon initiation of contraction.** Spheroplasts of cells expressing Rlc1p–GFP and Atb2–mCherry (**A**) or chd1-GFP (**B**) were made as described in the Materials and Methods and grown in minimal medium supplemented with 0.8 M sorbitol. Spheroplasts were mounted on agar pads with minimal medium and sorbitol and imaged using spinning disc confocal microscopy. Maximum intensity projections of the 3D section (0.6 μm step size) are shown. 39 of the 68 rings observed slipped to the pole of the cell instead of constricting centripetally. Scale bar: 5 μm.

will see later) features of these sliding dynamics are replicated in images of both myosin II (Fig. 1Ai–v) and F-actin (Fig. 1Bi–iii), thus identifying actomyosin contractility as the driving force for sliding. In many spheroplasts, ring constriction and sliding in the absence of septation led to additional cycles of ring assembly and disassembly (Fig. 1Bi; supplementary material Movie 6), which likely results from the maintenance of the cytokinesis checkpoint until completion of cell division (Le Goff et al., 1999a; Liu et al., 1999; Mishra et al., 2004). The sliding instability occurred even when the spheroplasts were not exactly spherical; in those with a conical shape, ring sliding was observed to proceed from the basal region of the cone towards the apex (Fig. 1Bi; supplementary material Movie 6). These observations suggested two possibilities: (1) the sliding dynamics of actomyosin rings were a consequence of geometry, i.e. rings slide along surfaces with decreasing cross sectional radius (spherical or conical cells) rather than undergoing constriction coupled with ingression; or (2) the lack of a cell wall in spheroplasts might lead to the destabilization of the position of the constricting actomyosin ring.

To distinguish between these possibilities, we investigated the behavior of contractile rings assembled in fission yeast cells that have a normal cell wall. To this end, we sought to misplace actomyosin rings to the hemispherical ends of cells that resemble WT cells in their morphology. If cell geometry was the cause of cortical ring instability rather than cell wall defects, then the contractile rings assembled at the hemispherical end-caps would slide during constriction. We imaged actomyosin ring behavior in cells defective in Mid1p, the anillin-related protein, which is important for division site positioning (Sohrmann et al., 1996; Bähler et al., 1998). Imaging *mid1*-18 temperature-sensitive mutant cells showed that actomyosin rings that assembled on hemispherical ends of the cells underwent sliding behavior (Fig. 2A). This sliding behavior was exacerbated by introduction of mutations in formins such as *for3*Δ. In *mid1*-18 *for3*Δ mutants (Fig. 2Bi–iii; supplementary material Movies 9–11) actomyosin rings assembled near the cell ends and underwent a sliding behavior. Notably, in these cylindrical cells (*mid1*-18 *for3*Δ), we also found that in every instance where misplaced rings

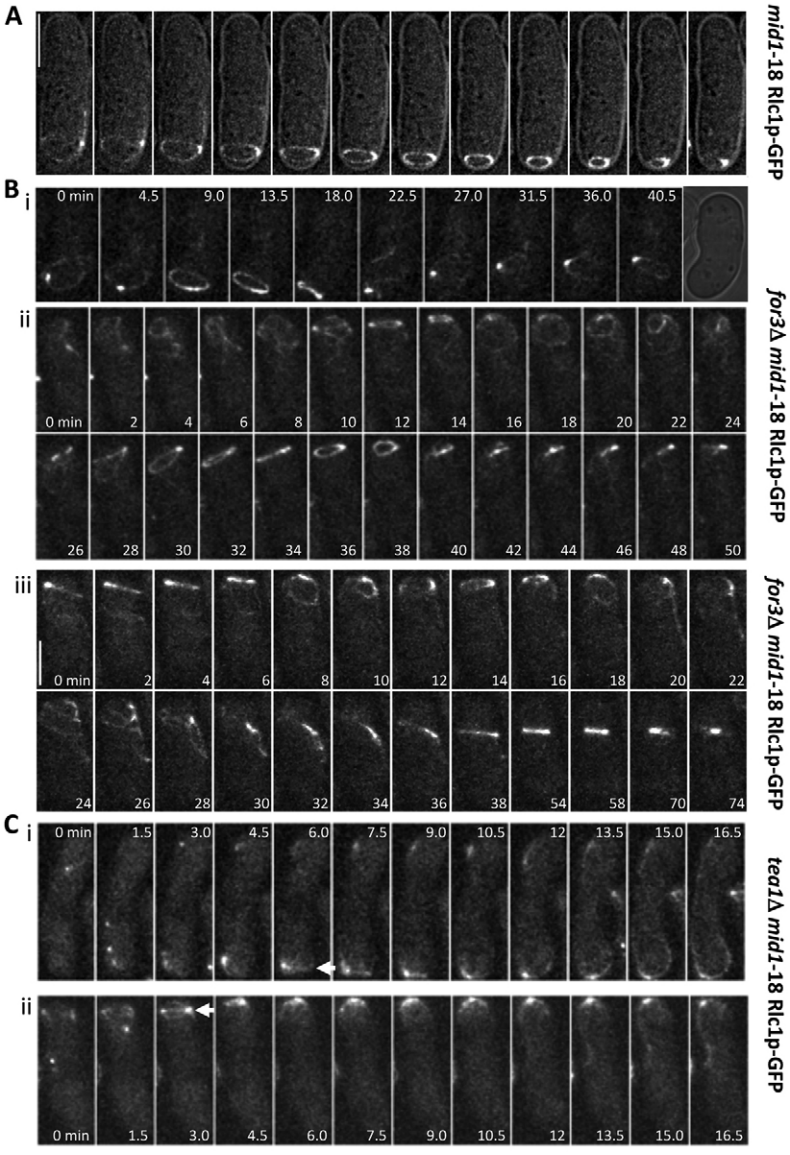


**Fig. 2. Slippage of actomyosin rings assembled at the hemispherical ends of cylindrical cells.** (**A**) *mid1*-18, (**B**) *for3*Δ *mid1*-18 and (**C**) *tea1*Δ *mid1*-18 cells expressing Rlc1p–GFP were grown in YES to exponential phase at 25℃, shifted to 36℃ for 4 hours. Such cells often showed actomyosin rings at the cell ends. Time-lapse microscopy of these cells showed actomyosin rings slip rather than constrict when assembled at the hemispherical ends of the cells. In *for3*Δ *mid1*-18 cells (Biii), when the actomyosin rings assembled at the hemispherical cells ends (time 0–28 min) such rings slipped along these hemispherical cell ends. However, when the actomyosin ring assembled at the cylindrical part of the cell (time 36 min) these rings were stabilized and underwent a successful contraction leading to division of the cell. The arrows in *tea1*Δ *mid1*-18 cells (Ci,ii) indicate the actomyosin rings assembled at hemispherical ends. LSM 510 confocal microscopy was used to perform 3D time-lapse (0.6 μm step size), and maximum projections are shown. Elapsed time is shown in minutes. At least six cells were imaged in each category. Scale bars: 5 μm.

assembled in the cylindrical regions ($n>5$), normal ring constriction and septation ensued (Fig. 2Biii).

The instability of the ring on the hemispherical ends of the cylindrical (*mid1*-18) cells could, however be attributed to presence of a protein complex comprising of Tea1p, Tea4p and Pom1p (tip complex), which is known to prevent anchoring of the actomyosin rings at the cell ends (Huang et al., 2007). To ensure that instability of the ring is due to the hemispherical shape and not due to presence of tip-complex, we imaged the actomyosin ring (Rlc1p-GFP) in *mid1*-18 *tea1*Δ (Fig. 2C) and *mid1*-18 *tea4*Δ cells (data not shown). We found that this consistently led to the anchoring of actomyosin rings to the extreme ends of the cell (Huang et al., 2007). However, prior to this attachment at the extreme cell ends, actomyosin rings slid down from the region of maximal cross-sectional diameter to the region of smaller cross-sectional diameter (Fig. 2C marked with arrows; supplementary material Movies 12, 13).

We next investigated whether actomyosin rings underwent sliding in spherical *orb6*-25 cells (Verde et al., 1998). Time-lapse imaging experiments showed that actomyosin rings slipped in 3 out of 20 cells (supplementary material Fig. S2Ai,ii), which is lower than that in WT spheroplasts as well as spherical end caps. Then, we investigated the position of the division septum in spherical *orb6*-25 cells held at the restrictive temperature of 36°C. Approximately 60% of spherical cells misplaced the division septum such that the post-mitotic nuclei were placed on the same side of the septum (supplementary material Fig. S2B), establishing that the spherical geometry affects the placement of the division site.

Our experiments on spheroplasts and cylindrical yeast cells using a variety of mutants (such as, *mid1* and *tea1*, *tea4* mutants) together established that cell geometry is an important factor in determining stability of the cortical ring. We further confirmed that, even within a single cell, rings that assembled in hemispherical regions underwent sliding, whereas those assembled in cylindrical regions underwent normal constriction and septation.

Having made this correlation between spherical geometry and actomyosin ring instability, we next sought to understand the physical basis of the dynamics of rings assembled within these spherical geometries. We made quantitative measurements of the ring dynamics and developed a theoretical model describing the dynamics of shrinking of the cortical ring driven by mechanical stresses generated by the contractile actomyosin ring, which have components along the tangent and normal to the cell surface. The active normal stress is balanced by membrane elastic stresses, while the active tangential stress is balanced by viscous stresses. Ingression occurs when the normal component of the contractile stress exceeds the membrane elastic stress. The osmotically tense spheroplasts are possibly too rigid for ingression to occur. On the other hand, the tangential components of the contractile stress cause the contractile ring to slide towards the poles. In most of the instances of ring sliding (supplementary material Movies 1–5, 9–13) the rings are coplanar and maintain their integrity until it approaches the poles. Analysis of the labeled myosin II images showed that the intensity of myosin is uniform along the circumference of the ring (Fig. 3A). In addition, the myosin II mean intensity per unit length of the ring was found to be roughly constant in time (Fig. 3B). This implies that for a contracting ring of fixed width (Fig. 3B), the myosin and filaments must turnover (discussed in a later section). Taking the contractile force density to be proportional to myosin concentration, these observations suggest that (1) the instantaneous position of the ring of radius $r(t)$ can be represented by a polar angle $\theta_0 t$; (2) the actomyosin contractile force density $f_r$ (force per unit length of ring) is uniform along the circumference of the ring; and (3) the actomyosin contractile force density is constant in time (Fig. 3C). Since during sliding the actomyosin contractile stress is balanced by the viscous

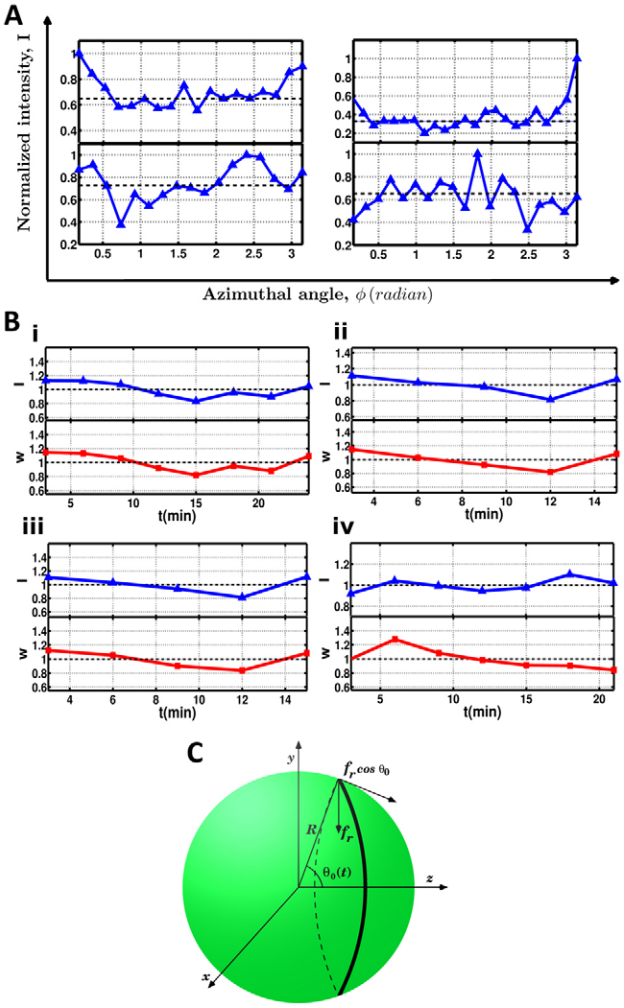


**Fig. 3. Testing the assumptions of the mechanical model from myosin II fluorescence images.** (**A**) Plot of Myosin II fluorescence intensity along the circumference of the ring parameterized by the azimuthal angle (in radians) for four spheroplast cells. The intensity $I$ is computed by first integrating the myosin II intensity over the ring width (defined as the scale over which the intensity falls by half of its maximum) and then binning over 5 pixels along the circumference of the ring. For convenience we normalize $I$ by its maximum value along the ring. These images show that the Myosin II fluorescence intensity (and hence the active contractile force) is uniform along the ring. Note that the higher intensity at the two ends is a result of projection effects. (**B**) Myosin II intensity ($I$) averaged over the ring circumference (blue) and the average ring width $w$ (red) as a function of time (min) for four spheroplast cells (i–iv). The time series is plotted by normalizing to its mean (represented by the horizontal black lines). These images show that the Myosin II fluorescence intensity I (and hence the active contractile force) per unit length of the ring and the ring width $w$ are roughly constant in time. (**C**) Schematic of contractile ring on the surface of spherical cell of radius $R$. The tangential component of contractile force per unit length is $f_r=\cos\theta_0(t)$, where $\theta_0(t)$ denotes the instantaneous angular position of the ring on sphere and can take values between $\frac{\pi}{2}$ to 0 corresponding to ring placed at equator and at the poles, respectively.

stress, we have $\gamma v_\theta = f_r \cos\theta_0$, where $\gamma$ is a ring friction coefficient and $v_\theta = R\dot{\theta}_0$, is the angular velocity of the ring (overdot represents time derivative) sliding along a cell of radius $R$. This relation immediately gives a time scale for sliding, $\tau_s = \frac{R}{\Lambda f_r}$, where $\Lambda$ is the mobility (inverse friction) per unit length of the ring. The equation for force balance can be easily solved to explicitly obtain the time dependence of the angular position of the ring,

$$\theta_0(t) = \frac{\pi}{2} - 2arc\cot\left[e^{-\frac{t}{\tau_s}}\cot\left(\frac{\pi}{4} - \frac{\theta_0(0)}{2}\right)\right], \qquad (1)$$

where $\theta_0(0)$ is the initial angular position of the ring.

Using this, we made a detailed comparison of the predictions of the theoretical model with experimental data on the sliding dynamics of contractile rings in spheroplasts and cell ends, as obtained from the fluorescence images of myosin II. In making this comparison we first noted that the equation for force balance implies that for a fixed cell radius, the angular velocity of the ring depends only on its instantaneous angular position. We made use of this feature to reorganize the data (angular position of the ring versus time) collected from cells of roughly the same radii (Fig. 4i,iii); the resulting data for the cell ends and spheroplasts collapsed along a master curve when plotted against time scaled by the sliding time $\tau_s = \frac{R}{\Lambda f_r}$ (Fig. 4ii,iv). The curves are well described by Eqn 1 for both spheroplasts and cell ends as seen by the fits to the experimental data (Fig. 4v,vii). Knowing $\tau_s$, and estimating $R$ from the cell images, we obtained a distribution of the characteristic velocity $\Lambda f_r$ across different cells. We found that this has a very narrow distribution centered about 0.12 μm/min and 0.17 μm/min for spheroplasts and cell ends, respectively (Fig. 4v,vii, inset). Since the origins of the ring friction and contractile force are very different, this suggests that the contractile force density in the ring is roughly constant in the cells, independent of their size. In particular, this means that the cells recruit the same number of myosin per unit length independent of its size. Further, since the characteristic velocity is independent of $R$, the measured slipping time $T$ (related to $\tau_s$) increases linearly with cell size (Fig. 4vi,viii).

We then addressed if the cylindrical morphology based ring maintenance anchoring played a physiological role in the fidelity of cytokinesis. To this end, we studied the behavior of actomyosin rings in conditions in which cell morphology is compromised to such an extent that sections of the cell cortex bulge out as a sphere. Cells lacking Myo52p, a non-essential type V myosin, lead to such shape abnormalities (Motegi et al., 2001; Win et al., 2001). In WT *S. pombe* cells with uniform cylindrical shape, septa are always positioned in the middle of the cell. Therefore, we first determined if this shape defect in *myo52*Δ had any consequence on septum position. While in the WT cells, only 3% of the cells have misplaced septa, almost 36% of the cells in *myo52*Δ had the septa positioned away from the middle (Fig. 5A–C). This implied that actomyosin rings, directed septation away from the mid-cell in the misshaped *myo52*Δ cells. This could be because the actomyosin rings assembled at non-medially located sites. However, yet another possibility is that the actomyosin ring was indeed assembled at medial positions, but due to the local spherical geometry of the cell, they were unstable and as predicted from the earlier experiments

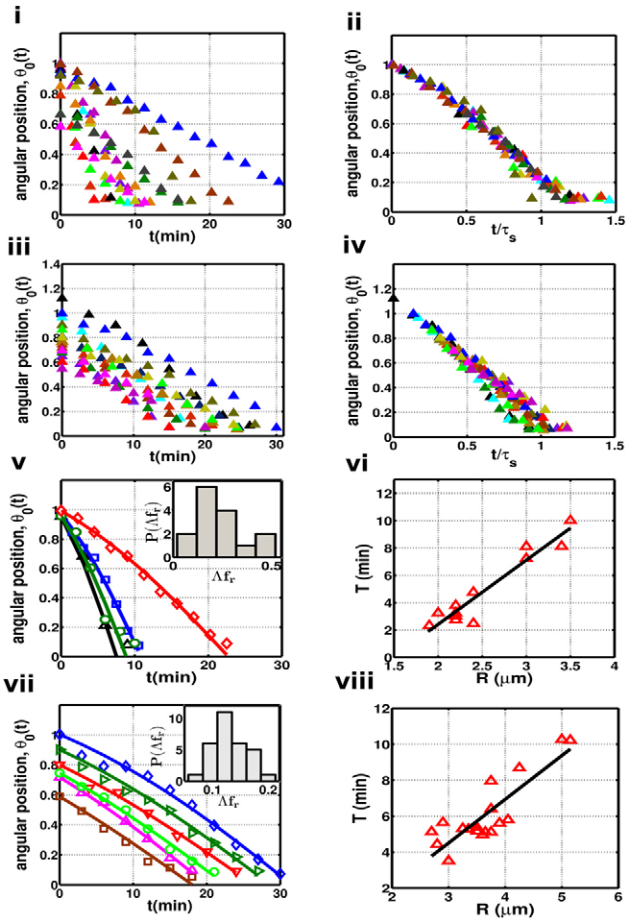


**Fig. 4. Comparison of predictions of mechanical model with experiments.** (**i**, **iii**) Angular positions (in radians) of the ring versus time (in minutes) for cell ends and spheroplasts (15 events each), respectively, obtained from the fluorescence images. We use Eqn 1 to reorganize the data in i and iii, because the angular velocity of the ring for cells of the same size, $R$ depends only on the instantaneous position of the ring, we can make relative shifts along the time axis to obtain a smooth profile of $\theta_0$ versus $t$ for each $R$. Each of the resulting data sets can then be fitted to the expression for the angular position versus time (Eqn 1) with $\tau_s$ as parameter. We use this value of $\tau_s$ to replot the data with respect to the scaled time $\frac{t}{\tau_s}$, this results in a collapse onto a master curve shown for cell ends (**ii**) and spheroplasts (**iv**). Plots for cell ends (**v**) and spheroplasts (**vii**) show the comparison of the experiments (data points) with predictions of the mechanical model, Eqn 1 (solid lines). From the fits to the data with different $R$, we extract the parameter $\tau_s$. The insets show the distribution of characteristic velocity $\Lambda f_r = \frac{R}{\tau_s}$, which are narrowly peaked about 0.17 μm/min for cell ends and 0.12 μm/min. (**vi**, **viii**) Linear scaling of slipping time $T$ (in min) to travel a fixed angular distance with the radius of the cell $R$ (in μm).

and the mechanical model, slipped down to more stable uniformly cylindrical regions of the cell. To distinguish between these possibilities, we imaged the assembly process of the actomyosin rings (labeled by CHD–GFP) (Karagiannis et al., 2005) through constriction by time-lapse microscopy in *myo52*Δ cells and compared it to the WT cells. As expected, in WT cells, actomyosin rings assembled at the mid-cell site and remained stable and constricted at the same location (Fig. 5Di,ii; supplementary material Movie 14). However, in the *myo52*Δ cells, although the actomyosin rings assembled at medial sites,

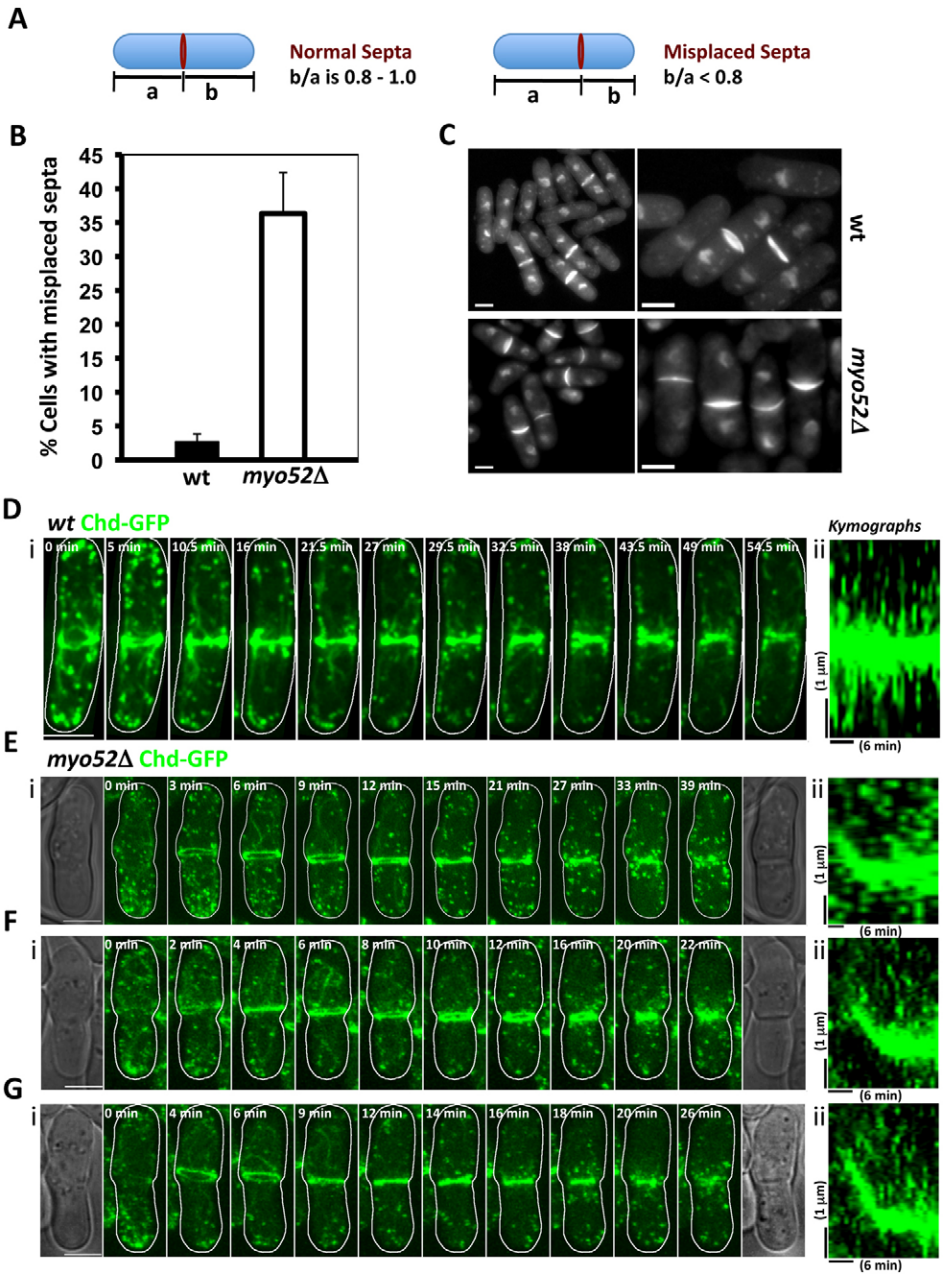


**Fig. 5. Misplacement of septa in *myo52*Δ cells and slippage of actomyosin rings in non-cylindrical regions along the cell axis.** (**A**) Schematic representation of septum position. The distance between the septa and two cell ends along the long axis of the cell was measured. The cells with a ratio of less than 0.8 between the short and long daughter were scored as cells with misplaced septa. (**B**) Quantification of misplaced septa in WT and *myo52*Δ cells. (**C**) Images of cells counted in B. Scale bars: 4 μm. (**D**) Time-lapse analysis of actomyosin ring assembly and constriction in WT cells expressing Chd1p–GFP (i) and kymograph of assembly and constriction period (ii). (**E**–**G**) Time-lapse of actomyosin ring assembly and constriction in *myo52*Δ cells expressing Chd1p–GFP (i) and kymograph of assembly and constriction period (ii). Cultures were grown in YES to exponential phase at 24℃, shifted to 36℃ for 4 hours and then imaged by Spinning disk confocal microscopy at 36℃. Maximum intensity projections of the 3D section 14 (0.5 μm step size) are shown. Elapsed time is shown in minutes. Time-lapse microscopy showed that actomyosin rings assembled in the non-cylindrical regions close to the cell middle and then slipped before beginning to constrict and ingress at the regions of constant diameter. Scale bars: 4 μm (D–G).

the rings were unstable in the regions with spherical geometry and slipped down (Fig. 5E–G; supplementary material Movies 15–17) in a process similar to that seen in spheroplasts and hemispherical cell ends. Interestingly, actomyosin rings stabilized as soon as they reached cylindrical regions of the cell and constricted. Thus, we conclude that local spherical geometry in cells lead to instabilities in cytokinetic actomyosin rings and compromise faithful cell division. These results, thus demonstrate the influence of cell geometry on the stability of the actomyosin rings and its physiological importance in the fidelity of the cytokinetic process.

## Discussion

In summary, we have shown that actomyosin rings in spheroplasts and hemispherical ends/local spherical regions of cylindrical cells spontaneously slide as soon as they assemble on the cell surface. Assembly and subsequent dynamics of the contractile ring is the result of complex interactions between actin filaments and myosin. However, under certain assumptions, which we verify experimentally, this sliding instability of actomyosin rings on locally spherical and conical geometries can be quantitatively understood using a simple mechanical model based on contractile forces exerted by the ring at the cell surface. The assumptions implicit in the simple mechanical model are that the contractile force density is (1) uniform along the ring and (2) constant in time. Our analysis of fluorescence images of myosin II in the constricting rings is consistent with these assumptions (Fig. 3A,B).

We verify several predictions from this model, in particular the dependence of the slipping time on cell size. In several instances of multiple assembly of contractile rings in cell ends (Fig. 2C), we see that the contractile ring slips whenever it assembles on a

locally spherical geometry, and stabilizes and constricts when it assembles on a locally cylindrical surface. Similarly, in *myo52Δ* cells (Fig. 5E–G), the contractile ring slips following assembly on a locally spherical part of the cell surface and stabilizes and constricts as soon as it encounters a local cylindrical surface. The width of the ring appears constant and the dynamics appears to change smoothly when the ring goes from a slipping to constriction behavior. While these changes need to be quantitatively dissected, this would suggest that the molecular processes involved in sliding and constriction are the same.

The good agreement between the simple mechanical model and experiments indicates that the turnover kinetics of myosin II is not rate limiting for the ring constriction. This can only happen if the filament and myosin turnover rate is high. We carried out fluorescence recovery after photobleaching (FRAP) experiments to estimate the turnover rate of myosin II in slipping rings spheroplasts. Myosin II was found to be highly dynamic with a $t_{1/2}$ of 16±3 sec ($n$=18). This turnover rate was comparable to those reported in intact cells that range from 12.9 sec to 30 sec (Pelham and Chang, 2002; Sladewski et al., 2009), which is much faster than the sliding rate. Interestingly, although our analysis points to the fact that myosin II concentration remains constant throughout constriction, previous work has shown that myosin II concentration increases during constriction in cells (Wu and Pollard, 2005). It is unclear if the differences may be attributable to the fact that in our studies we have investigated cytokinesis that is uncoupled with septation.

A crucial aspect that we revisit is the maintenance of the integrity of the ring. This implies that the contractile force density is uniform along the ring circumference, for were it not, different parts of the ring would have slipped with different angular velocities, leading to a disruption of the ring. Our measurements of the uniform distribution of myosin II from the images are consistent with this. How is this uniformity established and maintained given that the ring is assembled by the local recruitment of F-actin and myosin II? Are there molecular checkpoints that trigger constriction only after uniformity of force density is established – this seems unlikely in the context of spheroplasts. The more likely explanation is based on the fact that inhomogeneities in myosin recruitment lead to inhomogeneities in active contractile forces along the ring circumference, driving circumferential currents that quickly re-establish the homogeneity of the ring. The experiments with spheroplasts, cylindrical yeast cells and the physical description of the actomyosin dynamics on spherical geometries imply that the cytokinetic ring would inherently be unstable in a spherical region, unless anchored/fixed by ensuing septation or would require to be assembled in the cylindrical region which has a constant diameter.

The sliding behavior we observe is more rapid compared to that observed in septation-defective cylindrical cells treated with tubulin poisons (Pardo and Nurse, 2003). It is likely that the new membranes and septum, which are assembled concomitant with ring constriction play a role in maintenance of the position of the cell division site. The locally cylindrical geometry (having a constant cross-sectional diameter) might play a role in stabilizing the actomyosin ring such that actomyosin ring constriction leads to ingression of the cortex, rather than sliding of the ring. The fact that actomyosin ring sliding is not frequently observed in spherical mutants (compared with WT spheroplasts) suggests that in this situation, the anchoring of the ring due to the enhanced cell wall deposition can counterbalance the sliding instability induced by the spherical cell geometry (supplementary material Fig. S2) (Ge et al., 2005). On the other hand, actomyosin ring slippage is seen in nearly all cases where rings assemble at cell ends; an explanation consistent with the above is that here the anchoring due to the cell wall is not strong enough to counterbalance the actomyosin ring sliding. This suggests that the cylindrical geometry of the wild type cell facilitates maintenance of the actomyosin ring position for maximal fidelity of cytokinesis. Although fertilized eggs of Xenopus and sea urchins undergo division despite a spherical morphology, many other cell types generate a long and short axis (with a region of constant cross-sectional diameter or of negative curvature) prior to cytokinesis. It is noteworthy that the estimated turgor pressure in these cell types is at least 1000 fold lower than fission yeast (Kelly et al., 1997; Minc et al., 2009; Stewart et al., 2011). It is also possible that the actomyosin ring might interact more strongly with the cell cortex in metazoan eggs than in other cell types such as yeast. These factors may account for the difference in stability of actomyosin rings in these systems. Thus, symmetry breaking and the generation of a long and short axis with a region of constant cross sectional diameter or negative curvature might also play a role in the fidelity of cytokinesis in other cell types.

## Materials and Methods

### Yeast strains

The *S. pombe* strains used in this study were MBY5985 *mcherry-atb2::hph rlc1-3XGFP::kan*$^r$ *ura4* -D18h-; MBY2309 *JK148-nmt41-GFP-CHD::leu1+ ura4*-D18 *leu1*-32 *ade6*-216 h-; MBY1287 *mid1*-18 Rlc1p-GFP::ura4; MBY3580 *for3Δmid1*-18 Rlc1p-GFP::ura4; MBY2699 *tea1Δmid1*-18 Rlc1p-GFP::ura4; MBY6432 *orb6*-25 Rlc1p-GFP::ura4; MBY7159 *myo52A::ura4 leu1-32 ura4D-18 ade6-210 h+* (a gift from Dr Daniel Mulvihill); MBY7294 *myo52Δ* CHD-GFP.

### Yeast media and spheroplasting

Cells were grown in YES or minimal medium (Moreno et al., 1991). Cultures of *mid1*-18 Rlc1p-GFP, *for3Δ mid1*-18 Rlc1p-GFP, *tea1 Δ mid1*-18 Rlc1p-GFP, *orb6*-25 Rlc1p-GFP and *myo52Δ* were grown in YES at 24℃ until they reached an $OD_{595}$ of 0.3–0.5. Cultures were then shifted to 36℃ for 2–3 hours (*for3 Δmid1*-18 Rlc1p-GFP and *tea1 Δ mid1*-18 Rlc1p-GFP) or for 4 hours (*orb6*-25 and *myo52 Δ* before imaging. For spheroplasting cells were grown in minimal medium (MM) for 24 hours. The $OD_{595}$ of the culture was always maintained between 0.2–0.6. Cells were washed once in E-buffer (50 mM sodium citrate, 100 mM sodium phosphate pH 6.0) and re-suspended in E-buffer containing 1.2 M sorbitol. The cell suspension was adjusted to $5\times10^7$ cells/ml. Cells were incubated with lysing enzyme (L-1412; Sigma) at 36℃ for 10–30 minutes. Protoplast formation was monitored by phase contrast microscopy. Cells were washed with E-buffer containing 1.2 M sorbitol once 80–90% of cells were spheroplasted, followed by a wash with E-buffer containing 0.6 M sorbitol. Cells were then suspended in MM with 0.8 M sorbitol and grown with gentle shaking (80–90 r.p.m.) (Osumi et al., 1998). Cells were typically imaged four hours after spheroplasting.

### Microscopy

Cells were fixed with 3.7% formaldehyde and permeabilized with 1% Triton X-100 in PBS and stained with DAPI (DNA), Aniline Blue (cell wall) (Moreno et al., 1991). Live cells were imaged either on Zeiss Axiovest 200M microscope (Plan Apo 100× /1.4) equipped with a Yokogawa CSU-21 spinning disk system, Hamamatsu Orca-ER camera and driven by MetaMorph (v 7.6) software or on Zeiss LSM510 Meta confocal microscope. For time-lapse microscopy, exponentially growing cells were concentrated by low speed centrifugation (2000 r.p.m., 3 min) and resuspended in growth medium. 1 µl of cells were placed on slides with YES or EMM2 media containing 2% agarose pads, sealed under a coverslip using VALAP and imaged at the experimental temperature (Tran et al., 2004). Cultures of *myo52Δ* were imaged at 36℃. Images were analyzed with ImageJ software.

## Acknowledgements

Many thanks are due to Dr Masamitsu Sato for the mCherry-tubulin expressing yeast strain and Dr Daniel Mulvihill for the *myo52Δ* strain. We wish to thank members of M.B. and M.R. research groups for discussions and S. Ramaswamy for comments on the manuscript.

## Funding

M.R. was funded by an Human Frontier Science Program grant and Centre Franco-Indien pour la Promotion de la Recherche Avancée [grant number 3504-2]. M.B. acknowledges research support from the Singapore Millennium Foundation and the Mechanobiology Institute, Singapore. M.M. and R.S. were supported in part by a fellowship from the Singapore Millennium Foundation. N.S.G. thanks the Alvin and Gertrude Levine Career Development Chair; the Binational Science Foundation [grant number 2006285]; and Minerva [grant number 710589], for their support.

Supplementary material available online at
http://jcs.biologists.org/lookup/suppl/doi:10.1242/jcs.103788/-/DC1

## References

**Aspenström, P.** (2009). Roles of F-BAR/PCH proteins in the regulation of membrane dynamics and actin reorganization. *Int. Rev. Cell Mol. Biol.* **272**, 1-31.

**Bähler, J., Steever, A. B., Wheatley, S., Wang, Y., Pringle, J. R., Gould, K. L. and McCollum, D.** (1998). Role of polo kinase and Mid1p in determining the site of cell division in fission yeast. *J. Cell Biol.* **143**, 1603-1616.

**Balasubramanian, M. K., Bi, E. and Glotzer, M.** (2004). Comparative analysis of cytokinesis in budding yeast, fission yeast and animal cells. *Curr. Biol.* **14**, R806-R818.

**Chang, F. and Nurse, P.** (1996). How fission yeast fission in the middle. *Cell* **84**, 191-194.

**D'Avino, P. P.** (2009). How to scaffold the contractile ring for a safe cytokinesis - lessons from Anillin-related proteins. *J. Cell Sci.* **122**, 1071-1079.

**Fankhauser, C., Reymond, A., Cerutti, L., Utzig, S., Hofmann, K. and Simanis, V.** (1995). The S. pombe cdc15 gene is a key element in the reorganization of F-actin at mitosis. *Cell* **82**, 435-444.

**Ge, W., Chew, T. G., Wachtler, V., Naqvi, S. N. and Balasubramanian, M. K.** (2005). The novel fission yeast protein Pal1p interacts with Hip1-related Sla2p/End4p and is involved in cellular morphogenesis. *Mol. Biol. Cell* **16**, 4124-4138.

**Goode, B. L. and Eck, M. J.** (2007). Mechanism and function of formins in the control of actin assembly. *Annu. Rev. Biochem.* **76**, 593-627.

**Huang, Y., Chew, T. G., Ge, W. and Balasubramanian, M. K.** (2007). Polarity determinants Tea1p, Tea4p, and Pom1p inhibit division-septum assembly at cell ends in fission yeast. *Dev. Cell* **12**, 987-996.

**Karagiannis, J., Bimbó, A., Rajagopalan, S., Liu, J. and Balasubramanian, M. K.** (2005). The nuclear kinase Lsk1p positively regulates the septation initiation network and promotes the successful completion of cytokinesis in response to perturbation of the actomyosin ring in Schizosaccharomyces pombe. *Mol. Biol. Cell* **16**, 358-371.

**Kelly, S. M., Jia, Y. L. and Macklem, P. T.** (1997). Measurement of elastic properties of Xenopus oocytes. *Comp. Biochem. Physiol. A Physiol.* **118**, 607-613.

**Le Goff, X., Woollard, A. and Simanis, V.** (1999a). Analysis of the cps1 gene provides evidence for a septation checkpoint in Schizosaccharomyces pombe. *Mol. Gen. Genet.* **262**, 163-172.

**Le Goff, X., Utzig, S. and Simanis, V.** (1999b). Controlling septation in fission yeast: finding the middle, and timing it right. *Curr. Genet.* **35**, 571-584.

**Liu, J., Wang, H., McCollum, D. and Balasubramanian, M. K.** (1999). Drc1p/Cps1p, a 1,3-beta-glucan synthase subunit, is essential for division septum assembly in Schizosaccharomyces pombe. *Genetics* **153**, 1193-1203.

**Marks, J., Hagan, I. M. and Hyams, J. S.** (1986). Growth polarity and cytokinesis in fission yeast: the role of the cytoskeleton. *J. Cell Sci*. **Suppl. 5**, 229-241.

**Maupin, P. and Pollard, T. D.** (1986). Arrangement of actin filaments and myosin-like filaments in the contractile ring and of actin-like filaments in the mitotic spindle of dividing HeLa cells. *J. Ultrastruct. Mol. Struct. Res.* **94**, 92-103.

**Minc, N., Boudaoud, A. and Chang, F.** (2009). Mechanical forces of fission yeast growth. *Curr. Biol.* **19**, 1096-1101.

**Minc, N., Burgess, D. and Chang, F.** (2011). Influence of cell geometry on division-plane positioning. *Cell* **144**, 414-426.

**Mishra, M., Karagiannis, J., Trautmann, S., Wang, H., McCollum, D. and Balasubramanian, M. K.** (2004). The Clp1p/Flp1p phosphatase ensures completion of cytokinesis in response to minor perturbation of the cell division machinery in Schizosaccharomyces pombe. *J. Cell Sci.* **117**, 3897-3910.

**Moreno, S., Klar, A. and Nurse, P.** (1991). Molecular genetic analysis of fission yeast Schizosaccharomyces pombe. *Methods Enzymol.* **194**, 795-823.

**Motegi, F., Arai, R. and Mabuchi, I.** (2001). Identification of two type V myosins in fission yeast, one of which functions in polarized cell growth and moves rapidly in the cell. *Mol. Biol. Cell* **12**, 1367-1380.

**Naqvi, N. I., Wong, K. C., Tang, X. and Balasubramanian, M. K.** (2000). Type II myosin regulatory light chain relieves auto-inhibition of myosin-heavy-chain function. *Nat. Cell Biol.* **2**, 855-858.

**Osumi, M., Sato, M., Ishijima, S. A., Konomi, M., Takagi, T. and Yaguchi, H.** (1998). Dynamics of cell wall formation in fission yeast, Schizosaccharomyces pombe. *Fungal Genet. Biol.* **24**, 178-206.

**Pardo, M. and Nurse, P.** (2003). Equatorial retention of the contractile actin ring by microtubules during cytokinesis. *Science* **300**, 1569-1574.

**Pelham, R. J. and Chang, F.** (2002). Actin dynamics in the contractile ring during cytokinesis in fission yeast. *Nature* **419**, 82-86.

**Pollard, T. D. and Wu, J. Q.** (2010). Understanding cytokinesis: lessons from fission yeast. *Nat. Rev. Mol. Cell Biol.* **11**, 149-155.

**Schroeder, T. E.** (1973). Actin in dividing cells: contractile ring filaments bind heavy meromyosin. *Proc. Natl. Acad. Sci. USA* **70**, 1688-1692.

**Sladewski, T. E., Previs, M. J. and Lord, M.** (2009). Regulation of fission yeast myosin-II function and contractile ring dynamics by regulatory light-chain and heavy-chain phosphorylation. *Mol. Biol. Cell* **20**, 3941-3952.

**Sohrmann, M., Fankhauser, C., Brodbeck, C. and Simanis, V.** (1996). The dmf1/mid1 gene is essential for correct positioning of the division septum in fission yeast. *Genes Dev.* **10**, 2707-2719.

**Stewart, M. P., Helenius, J., Toyoda, Y., Ramanathan, S. P., Muller, D. J. and Hyman, A. A.** (2011). Hydrostatic pressure and the actomyosin cortex drive mitotic cell rounding. *Nature* **469**, 226-230.

**Tran, P. T., Paoletti, A. and Chang, F.** (2004). Imaging green fluorescent protein fusions in living fission yeast cells. *Methods* **33**, 220-225.

**Verde, F., Wiley, D. J. and Nurse, P.** (1998). Fission yeast orb6, a ser/thr protein kinase related to mammalian rho kinase and myotonic dystrophy kinase, is required for maintenance of cell polarity and coordinates cell morphogenesis with the cell cycle. *Proc. Natl. Acad. Sci. USA* **95**, 7526-7531.

**Win, T. Z., Gachet, Y., Mulvihill, D. P., May, K. M. and Hyams, J. S.** (2001). Two type V myosins with non-overlapping functions in the fission yeast Schizosaccharomyces pombe: Myo52 is concerned with growth polarity and cytokinesis, Myo51 is a component of the cytokinetic actin ring. *J. Cell Sci.* **114**, 69-79.

**Wolfe, B. A. and Gould, K. L.** (2005). Split decisions: coordinating cytokinesis in yeast. *Trends Cell Biol.* **15**, 10-18.

**Wu, J. Q. and Pollard, T. D.** (2005). Counting cytokinesis proteins globally and locally in fission yeast. *Science* **310**, 310-314.

Journal of Cell Science